J Nanostruct 15(1): 32-42, Winter 2025

RESEARCH PAPER

Role of Ag/ZnO Nanoparticles for Removal of Pollutants from Aqueous Solutions: Characterization and Environmental Applications

Elaph Salih Hadi *, Khawla. K. Jasim

Department of Chemistry, College of Science, University of Al-Muthanna, Al-Samawah, Iraq

ARTICLE INFO

Article History:
Received 08 September 2024
Accepted 20 December 2024
Published 01 January 2025

Keywords:
Ag-doped ZnO NPs
Brilliant blue BB dye
Hydrothermal method
Zinc oxide

ABSTRACT

ZnO nanoparticles (NPs) are effectively produced using a straightforward, efficient, high-yield, and inexpensive mechanochemical combustion process at various calcination temperatures. The impact of calcination temperature on ZnO nanocomposites' crystallinity has been investigated using X-ray diffraction (XRD). The synthesized ZnO and Ag/ZnO's XRD patterns show a well-crystalline wurtzite ZnO crystal structure. The ZnO NPs peak position obtained at 300–600 ◦C calcination temperatures is nearly identical to the peak position of ZnO obtained at a temperature without calcination. This paper has discussed the hydrothermal method of ZnO NPs production and photodepostion of Ag-doped ZnO NPs. Additionally, the behavior of the ZnO and Ag/ZnO nanocomposites is thoroughly examined in relation to the effects of calcination temperature on Transmission Electron Microscopy (TEM), Field Emission-Scanning Electron Microscopy (FE-SEM), Energy Dispersive Spectroscopy (EDS), and the measurement of specific surface area using the Bruner, Emmett, and Teller method.The absorption efficiency changed from 99.87% to 72.55% when the concentration of BB dye was increased from 10 to 50 ppm. Increasing the intensity of the UV light will improve the photocatalytic degradation and absorbance efficiency (PDE%) efficiency because the catalyst will receive more radiation, which will lead to the production of more hydroxide radicals .The photocatalytic efficiency increases from 77.7% to 97.7% in 1 h.

How to cite this article
Hadi E., Jasim K. Role of Ag/ZnO Nanoparticles for Removal of Pollutants from Aqueous Solutions: Characterization and Environmental Applications . J Nanostruct, 2025; 15(1):32-42. DOI: 10.22052/JNS.2025.01.004

INTRODUCTION

Industry play main role in the providing human necessity and enhancing their life style. However, some of industrial activities has negative repercussion becuse it because it presents hazards and affects the environment [1, 2] .Due to existence unfavorable chemical dyes in industry effluents cannot be ignored [3] .Dyes are chemical aromatic substances that add color by bond to surfaces and dyes are indispensable substances in the textile, pigment dies, paint, dyeing cosmetic, papers, plastics, and pharmaceutical manufacturing [4]. It is reported that about 15% of dyes are releasedo to the environment during dying processes [5-7]. Especially,organic dyes. Dyes have caused grave concern in scientific society as they not only give unaccept-able color and smell to water but also some of them are very poisonous and produce

* *Corresponding Author Email: elaphsalihhadi@gmail.com*

many other toxic to living organisms directly or indirectly by products during their long stay in water bodies owing to their non-biodegradable nature [8-10]. This pollutants should be destroyed or converted into harmless chemical substances By using chemical, physical, and biological techniques include ion exchange,bio-degradation, precipitation, reverse osmosis, coagulation and flocculation [11, 12].Some of these treatments mentioned above have a major disadvantage of simple transferring the pollutants from one phase to another phase rather than destroying them , which consequently lead to secondary pollution [13].

photocatalysis with semiconductors is a famous modern and rapid water treatment technology· It has many advantages such as low energy-consumption, high efficiency, extensive applicability , moderate condition, and decrease in secondary pollution [14].

In the present work,we used nanoparticles semiconductors as photocatalyst surface. Researchershavebecomeattentiveinnanoparticles of sizes between 1 and 100 nm for their chemical, optical, and mechanical characteristics [15]. When a material moving from micro particles to nanoparticles can be seen a noticeable change in the physical properties of this material. Two of the major factors that demonstrate these changes are the increasing in surface-to-volume ratio, and the particle size moving into the dominion where quantum confinement prevails [16, 17].

ZnO will play an influential role in the treatment of contaminationhas gained a considerable attention due to its wide band gap about (3.37ev). ZnO is a nontoxic with premium chemical and thermal stability and has an individual optical, semiconducting, electric conductivity, chemical sensing, and piezoelectric characteristics [18]. Photocatalytic for environmental treatment is One of the most important applications of ZnO nanoparticles . The pollutants react with ZnO nanoparticles at the particles surface and the efficiency of the photocatalytic property is depends on the shape, size and growth method of the crystals. The studies showed that the controlling of surface morphology could be enhancing the photocatalytic activity of ZnO nanoparticles [19]. Doping process has ability to absorb photons of light with a widening range of the solar spectrum. The photocatalytic activity of ZnO nanoparticles was enhanced using diverse dopants such as Ag. Ag Nano participle shows individual properties in chemical such specific chemical stability , conductivity which could be ideal hyberdization with ZnO with varieties in properties such,electronic conductivity , unique internal structure, and high surface area make it one of the best carbon materials to improve the properties of ZnO[20] . AgNPs optimize the behaviour of ZnO due to the abilities for prevents the recombination of electrons and holes and as

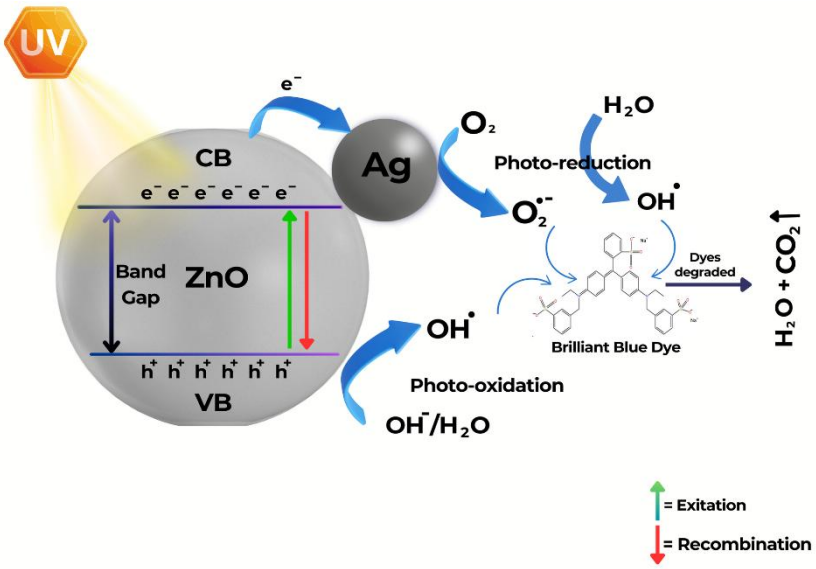

Fig. 1. Explained the mechanism of photocatalytic degradation process of (Ag/ZnO).

a result of prevent the agglomerations and that provided many active site for ZnO. In recent years research has been intensely centered around the preparation of ZnO nanoparticles using different conditions and methods, due to the properties which can be changed of metal oxide particles depending on track of preparation [21]. In the present work, Zno nanoparticles prepared by hydrothermal method and then synthesis Ag/Zno NPs by photodeposition technique .Here we report the photocatalytic degradation of BB dye with ZnO and the effect of operational parameters such as Calcination temperature ,the initial dye concentration , catalyst loading, and light intensity were studied to optimize the process for maximum degradation (Fig. 1).

The hydrothermal method was used by Radhi groups to create ZnO NPs. The chemical, optical, and mechanical properties of nanoparticles with sizes ranging from 1 to 100 nm have drawn the attention of researchers [22]. In the current work, Ag/ZnO NPs are synthesized via photodeposition approach after ZnO nanoparticles are generated by hydrothermal method.Here, we describe the photocatalytic degradation of brilliant blue dye using ZnO. To maximize the process's degradation, we evaluated the effects of several operational factors, including catalyst loading, initial dye concentration, calcination temperature, and light intensity.The synthesis of undoped and Ag-doped ZnO nanocomposites using the hydrothermal technique for ZnONPs and photodepostion for Ag/ZnONPs has been covered in this article. The behavior of ZnO and Ag/ZnO nanocomposites is examined in depth with regard to the effects of calcination temperature on X-ray diffraction (XRD), Transmission Electron Microscopy (TEM), Field emission-Scanning electron microscopy (FE-SEM),

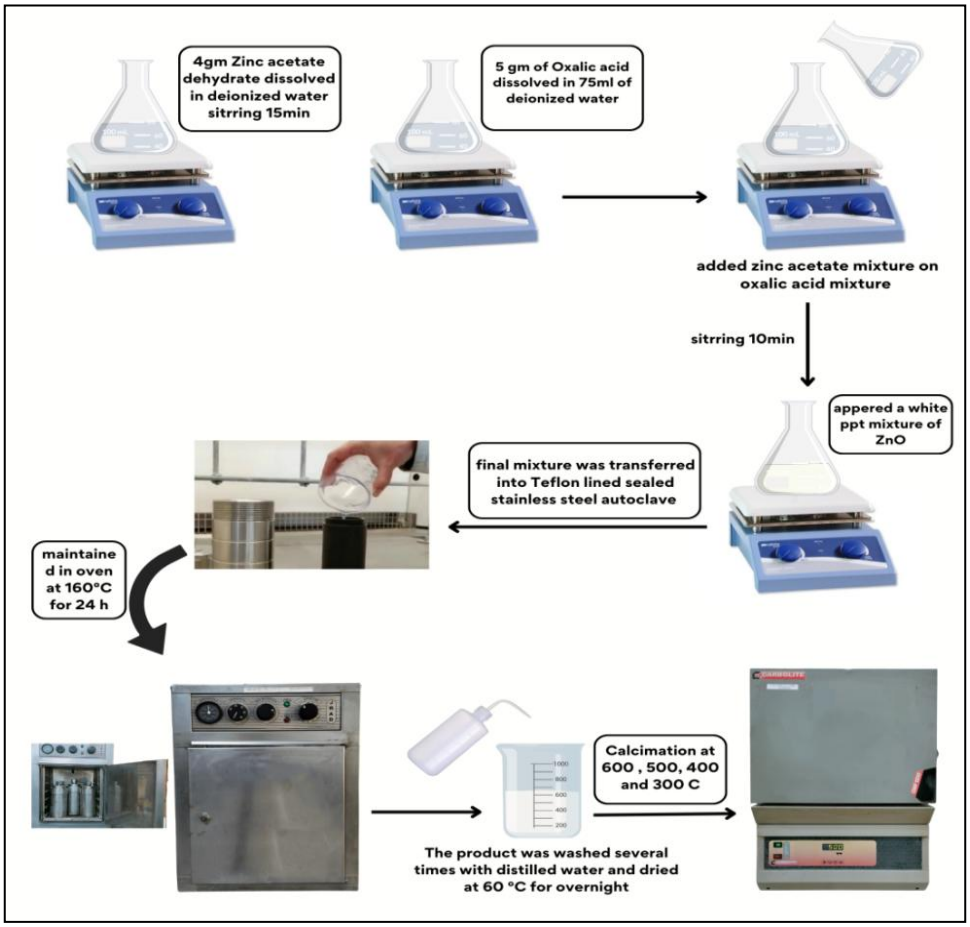

Fig. 2. Preparation of ZnO nanoparticle by hydrothermal method.

and Energy Dispersive Spectroscopy (EDS).

MATERIAL AND METHODS

Chemical and reagents

Loba Chemie, Scharlau, and Sigma-Aldrich-India provided all of the analytic-grade chemicals and reagents used in this study. The solution was prepared using deionized water.

Synthesis of ZnO nanoparticle

The hydrothermal approach was used to create zinc oxide nanoparticles. First, weigh out 4 grams of zinc acetate ($Zn(CH_3COO)_2$. $2H_2O$) and place it in a beaker. Then, dissolve it in 75 milliliters of deionized water. Next, dissolve 5 grams of oxalic acid ($C_2H_2O_4$) in 75 milliliters of deionized water in a different beaker.

Add the contents of the two beakers together with the subsequent chemical reactions. ZnO should form a colloid after zinc acetate is completely hydrolyzed in water with oxalic acid $H_2C_2O_4$.The resultant mixture was put into a 100 ml stainless steel container lined with Teflon [23] (the autoclave) after that ,the autoclave was placed inside the oven and tempterature of oven was set to 160 °C for 24 h .

The substrate was removed from the autoclave, cleaned several times with distilled water, and dried in an oven at 60 °C when the autoclave naturally cooled to room temperature. The goods were then further calcined for two hours at various temperatures in the air. Fig. 2 provided a description of this procedure .

Preparation of Metal Doped ZnO Nanocomposites

Metal doped zinc oxide was created by put (0.5 gm) of zinc oxide powder in (100 ml) of distilled water and stir for 5 min ,and add various volumes of $AgNO_3$ (0.1, 0.2, 0.3, 0.5,1 and 2) ml was used, mass ratio of Ag : 0.5–10 wt% then subjecting the mixture's surface to nitrogen gas for five more mints [24]. Subsequently, the combination was exposed to a light intensity of 1.68 $mW.cm^{-2}$ (using a UVA LED lamp) for the whole night, as illustrated in Fig. 3. Following radiation, the resulting powder was repeatedly cleaned with distilled water and allowed to dry overnight at 60°C in an oven.

RESULTS AND DISCUSSIONS

Characterizations of synthesized nanocomparticle

X-ray diffraction of metal oxide ZnO and Ag-ZnO nanocomposite

For characterizing crystalline materials, X-ray diffraction is a very efficient non-destructive technique. ZnO that has been calcined at (300,400,500,600) °C and ZnO that has not been calcined are depicted in Fig. 4 along with their XRD patterns. The ZnO NPs peak location recorded at calcination temperatures between 300 and 600 ◦C is nearly identical. The ZnO peak notation achieved

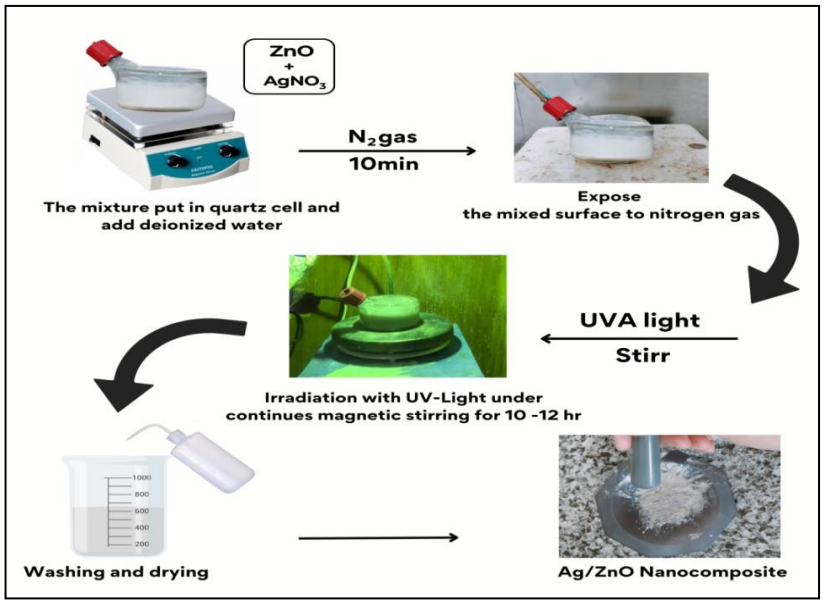

Fig. 3. Preparation of Ag/ZnO nanocompsite.

at no calcination.

Fig. 4 : Impurities are eliminated and crystallinity is enhanced following calcination at (300,400,500,600) °C without calicenation for ZnO. All the ZnO peaks were found to be sharper from (300 to 600)°C, indicating that crystal formation happens at higher calcination temperatures. The crystalline peaks of the ZnO nanoparticles are located at (31.6°, 34.4°, 36.2°, 47.4°, 58.6°, 64.8°, and,70°). correspond to the (100), (002), (101), (102), (110), (103), (200), (112), and (201) reflection planes, respectively. All the diffraction peaks can also be well indicate to the hexagonal Wurtzite structure of ZnO JCPDS card (no. 36-1451) [25].

The average crystallite size (dcryl) was calculated using the prominent peaks from Debye-Scherrer's formula:

$$D = \frac{K\lambda}{B\cos\theta} \quad (1)$$

where, D = particle size, θ = angle of diffraction, K= Scherer constant (=0.9), λ= x-ray wavelength, B = full wide that half maximum (FWHM) that is measured in radian [26] . were average crystallite size found to be 53.6771 nm ,21.53 nm, 22.4657 nm, 28.892 and 33.3514 nm for the ZnO without calcination and nanocatalysts calcined at 300˚C, 400˚C, 500˚C and 600 °C respectively. It can be noted that increase in temperature produced larger crystallite size Potti and Srivastava have reported that the crystallite size of the oxides expanded with increasing the calcination temperatures [27] due to the merger of smaller crystallites into bigger ones caused by high calcination temperatures [28-31].

A representative XRD pattern of Ag/ZnO nanoparticles is shown in Fig. 5. The diffraction peaks appearing at 31.7, 34.4, 36.2, 47.4, 56.5, 62.7, 66.3, 67.8 and 69.1° match the crystal plane of a wurtzite structure of ZnO and are comparable to literature values, JCPDS card (no. 36-1451). Furthermore, all diffraction peak positions of ZnO in Ag/ZnO composite accord with that of pure ZnO, indicating that Ag did not incorporate into the lattice of ZnO but dispersed on the surface of the ZnO nanoparticles. Therefore, the deposition of Ag does not affect the crystal or phase structure of ZnO. Metal islands deposited on the semiconductor surface have been shown to effectively trap the electrons promoted to the conduction band and thus the free holes formed in the valence band can participate in oxidation reactions.

The crystal sizes of all of the samples were estimated using the Scherrer equation. The average sizes of the Ag/ZnO nanoparticles, calculated by the Scherrer formula, were estimated to be

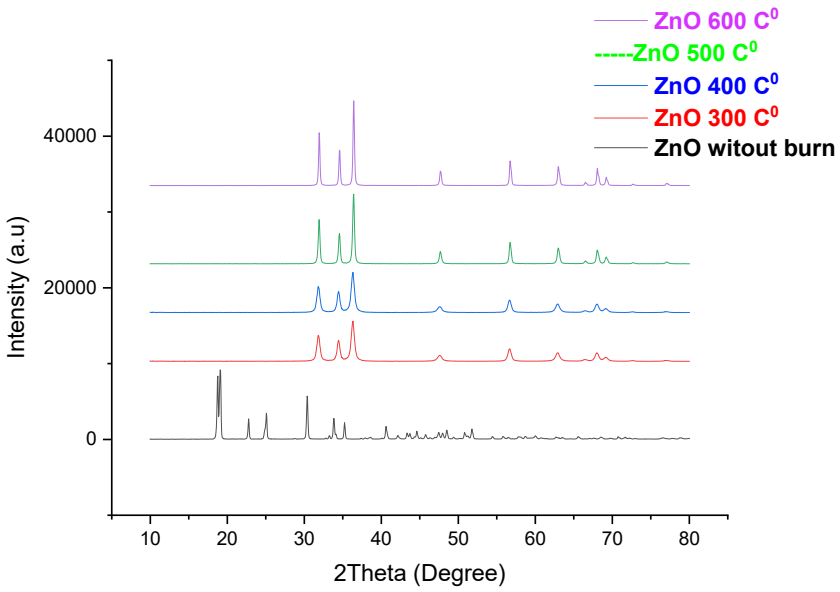

Fig. 4. X-ray diffraction patterns of nascent and calcinated ZnO NPs from (300-500) °C and without burn.

between 22 and 27 nm. The crystal size of the samples are calculated to be about 27.8, 27.21, 26.6, 25.3, 24,51 , 22.17 nm for 0.5 wt%, 1 wt% ,1.5 wt % , 2.5 wt % , 5 wt % and 10 wt% Ag/ZnO, respectively. The size decrease could be caused by lattice deformation associated with oxygen vacancies in the anatase crystallites, which may hinder crystallite growth. Nonetheless, there is no remarkable change in the *d* space values, which implies that the noble metal silver modification does not change the average unit cell dimension in deposited samples [32]. The absence of reflection from the silver deposits can be attributed to the low percentage deposition.

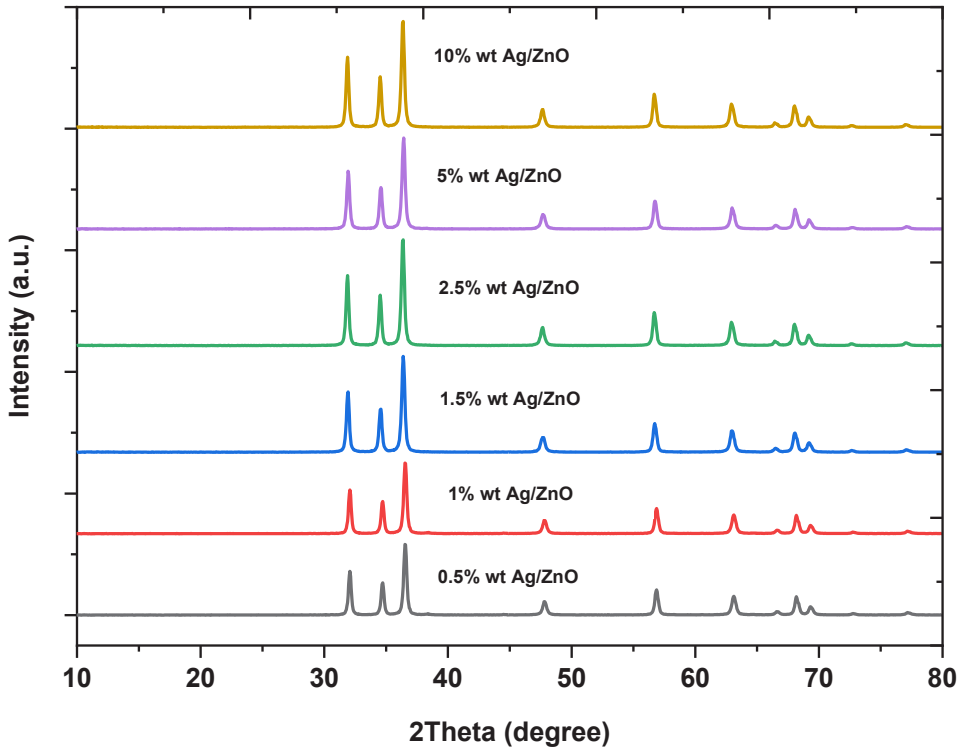

Fig. 5. XRD patterns of ZnO and various wt % of Ag modified ZnO sample.

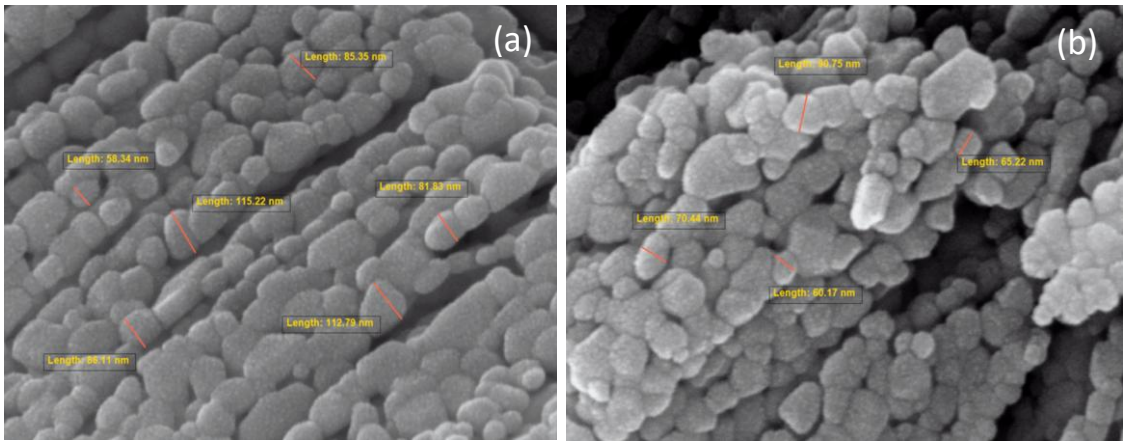

Fig. 6. FESEM image of a) ZnO NPs and b) Ag/ZnO nanocomposit

Field emission- Scanning electron microscopy(FE-SEM) and Energy dispersive spectroscopy (EDS)

Using the SEM technique, the surface morphology of pure ZnO nanoparticles has been investigated with respect to the size, shape, and distribution of the individual particles as well as any clusters that may exist within them. The SEM picture of ZnO, obtained after hydrothermal preparation and calcination at 500 °C for two hours, is displayed in Fig. 6 a-b. The nanoparticles exhibit a rod-like form, with a mean size ranging from 58 to 112 nm and a high degree of agglomeration.

As shown in Fig. 6b, FE-SEM image for Ag/ZnO describes the creation of a closely stacked cluster comprising rod-like with much agglomeration and their particle size ranges from around (60-90) nm. It has been noted that the rod-shaped photocatalyst is particularly effective at degrading organic dyes [33]. Images of Ag/ZnO obtained using field emission scanning electron microscopy show that when silver nitrate is injected during the reaction, the ZnO's shape changes from a rod shape to a smaller aggregation shape.

Dispersive energy spectroscopy The existence of ZnO and Ag-ZnO was confirmed by EDS. Ag-ZnO nanocomposites and the ZnO nanocrystal line exhibit strong and precise diffraction peaks, indicating good crystallinities. EDS spectra reveal

Table 1. EDS analysis of the ZnO and, Ag/ZnO nanocomposites' composition.

Sample	Zn Atomic %	O Atomic %	C Atomic %	Ag Atomic %
ZnO	24.48	27.91	47.61	0
Ag- ZnO	13.21	25.01	61.27	0.51

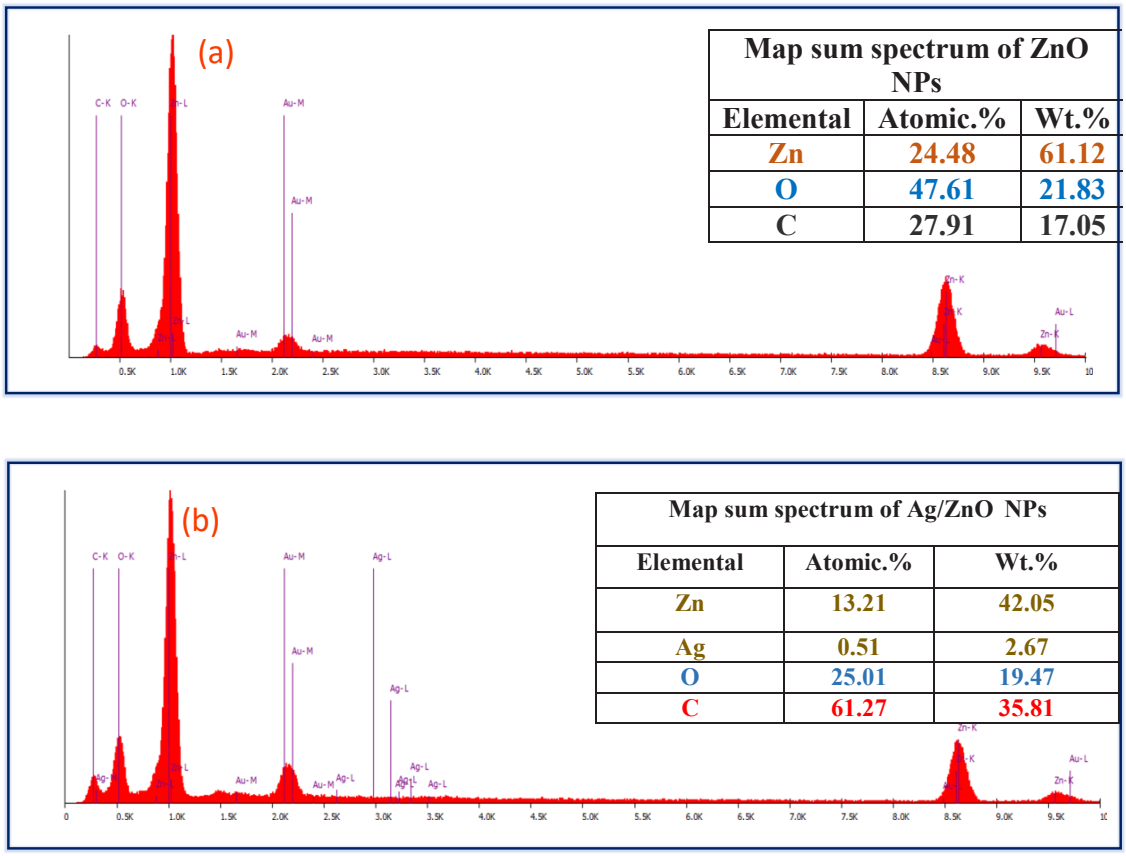

Fig. 7. EDS analysis and elemental mapping of pure (a) ZnO and, (b) Ag/ZnO nanocomposites.

that the only elements present in pure ZnO and Ag-ZnO nanocomposites are Zn, Ag, and O.

Table 1 presents a semi-quantitative assessment of the atomic concentration (atom%). It indicates that the products' carbon (C), zinc [10], oxygen (O), and silver (Ag) content for the ZnO and Ag-ZnO elements are 24.48, 27.91, and 47.61 and 13.21 %, 0.51%, 25.01 %, and 61.27%, respectively.

The EDS results are shown in Fig. 7, which makes it evident that the weight ratios of ZnO and Ag-ZnO NPs were 78.17% and 64.19%, respectively. The EDS examination showed that the sample contained the necessary phases of Zn and O and that the produced ZnO and Ag-ZnO NPs were highly pure. Similar Zn, O, and Ag ratios that are near to the theoretical values are seen in the EDS results from the current investigation.

The EDS data as shown in Fig. 7., which unambiguously show that the weight ratios of ZnO and Ag-ZnO NPs were 78.17% and 64.19%, respectively. The sample included the necessary phase of Zn and O, according to the EDS analysis, which also showed that the manufactured ZnO and Ag-ZnO NPs were highly pure. Zn, O, and Ag ratios in the EDS results from this investigation are comparable and nearly match the theoretical values. [34, 35].

Surface area and porosity analysis

The BET analysis is not consistent with the low mass concentrations of nanoparticles, which are typically in the range of 0.1 mg/m^3 or less [36]. The ZnO and Ag/ZnO samples had surface areas of 9.122 and 21.999 m^2 g^{-1}, respectively, according to Table 2.The BET measurement shows that the ZnO has a relatively small surface area.ZnO and Ag/

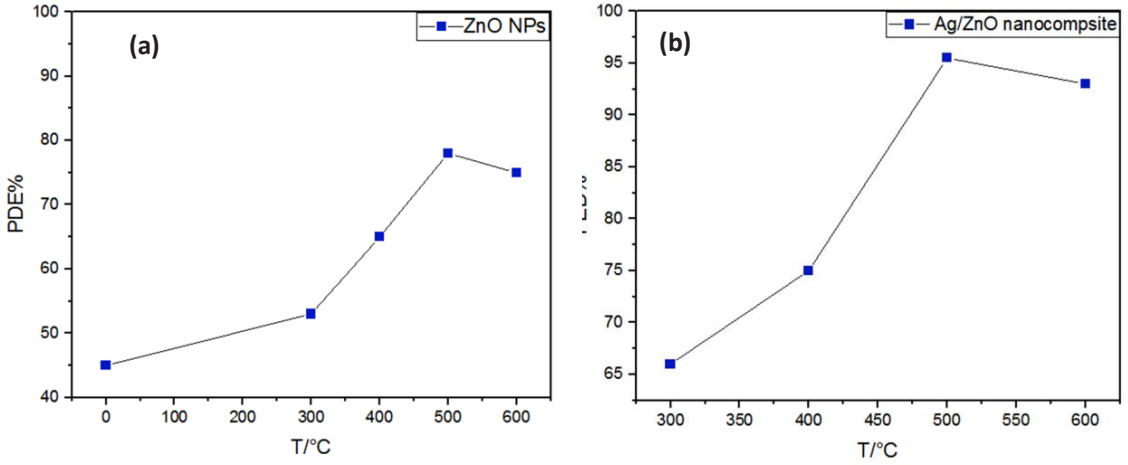

Fig. 8. Effect of different annealing temperatures on Photocatalytic efficiency of synthesized samples (a) Absorbance efficiency in presence of ZnO NPs as catalyst (b) Absorbance efficiency in presence of Ag/ZnO NPs as catalyst.

Table 2. BET analysis results of ZnO and Ag/ZnO NPs.

Surface physical parameters	ZnO NPs	Ag/ZnO NPs
BET surface area (m^2/g)	9.122	21.999
Pore diameter (nm)	62.56	26.877
Pore volume (cm^3 /g)	0.1899	0.143
Type of pore	Micro-porous	Micro-porous
Hysteresis (p/p°)	H3	H3

ZnO have total pore volumes of 0.1899 and 0.143 cm3 g-1, respectively.

Additionally, when the nanomaterials exhibit in the 35.683 nm range after being inoculated with silver nitrate via the photo deposition procedure, the pores' diameter reduces.

measured BET surface area of the sample ZnO was smaller than Ag/ZnO which can be correlated to the fact that the method of preparation helped to form a nanocomposite distinguished by its physical and chemical properties.

Effect of different parameters of photodeposition processes of Ag/ZnO nanocomposites onto Brilliant Blue dye

Effect of calcination temperature

The purpose of this study was to elucidate how the temperature of calcination affected the photolysis efficiency of Ag/ZnO nanocombsite and produced ZnO NPs. Fig. 8 displays the rates of Brilliant blue dye degradation in relation to various calcination temperatures.

The ZnO nanoparticles were calcined at temperatures ranging from 300°C to 600°C many times. was examined at 0.3 g from every produced sample, with a dye concentration of 30 ppm, and light intensity of 1.68 mW/cm^2. Since the size of the crystallites increased as the calcination temperature rose from 300°C to 500°C, the synthesized samples' photocatalytic activity increased simultaneously.

The change in the size and particle morphology of the ZnO and Ag/ZnO surfaces is responsible for the maximum photocatalytic efficiency at 500°C [24]. At 600°C, the photocatalytic activity slightly decreased; the lower photocatalytic activity of Brilliant Blue may be explained by the reduced amount of photo-generated electrons and holes that participated in the reaction [37]. Fig. 8-a illustrates how absorbance efficiency (PDE%) rises to approximately 78% at 500°C after calcination from 55% at 300°C and falls to 75% at 600°C. Fig. 8-b illustrates the impact of adjusting the annealing temperature. It shows that the absorbance efficiency (PDE%) increased from 63% at 300°C to 77% at 400°C, reaching a high of almost 96% at 500°C before declining slightly to roughly 94% at 600°C.

Selectivity of the Best Photocatalyst Surface

Electron-hole pair recombination is inhibited and optical efficiency is enhanced by the Ag concentration. Because they produce a Schottky barrier when they come into contact with metallic semiconductors, noble metal nanoparticles placed on the surface of zinc oxide (ZnO) are known to function as efficient traps for photogenerated electrons.

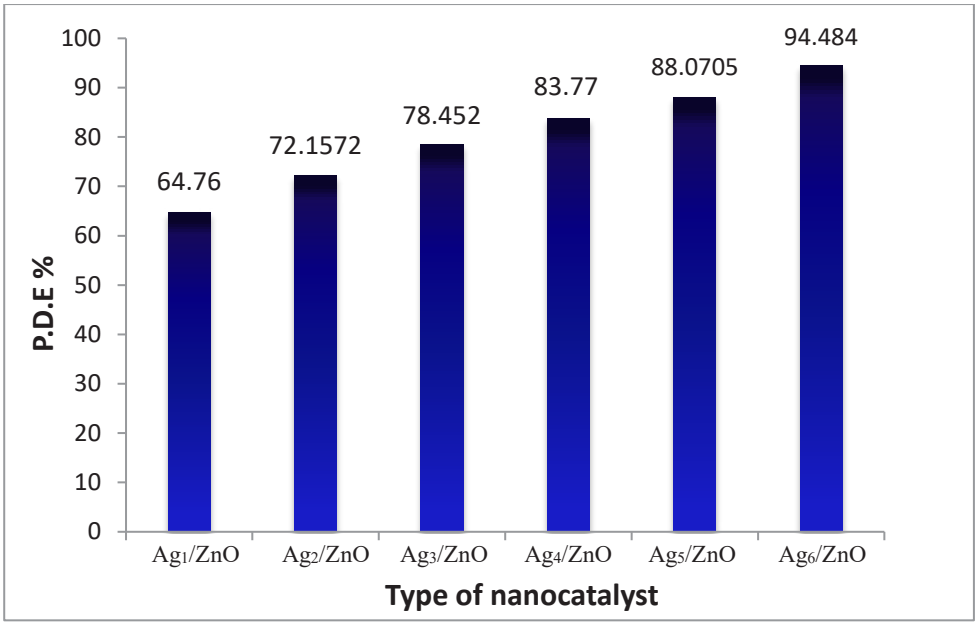

Fig. 9. Selectivity of the best photocatalyst surface PDE% with a type of nanocatalyst.

These electrons stop electron-hole recombination and speed up the reduction of oxygen [38]. ZnO and Ag nanoparticles come into contact under light, and as the two systems approach equilibrium, the photogenerated electrons are shared between the two kinds of particles. This process is known as electron transfer from excited ZnO to Ag.

The electron accumulation of the Ag particles increases the Fermi level to a more negative potential, which also causes a shift in the Fermi level of the compound closer to the conduction band of the composite [39].

In Fig. 9: To examine how the Ag content affects the photocatalytic activity of Ag/ZnO nanocomposites to breakdown Brilliant blue dye, a number of $AgNO_3$ volumes were carefully selected. We add 0.1, 0.2, 0.3, 0.5, 1, and 2 milliliters of $AgNO_3$ to ZnO NPs in this experiment, mass ratio of Ag : 0.5, 1, 1.5 ,2.5 , 5 , 10 wt% and we designate the generated nanocomposites as Ag_1/ZnO, Ag_2/ZnO, Ag_3/ZnO, Ag_4/ZnO, Ag_5/ZnO, and Ag_6/ZnO, respectively.The (Ag/ZnO) amount was 0.3 g, and the light intensity was 1.68 mW/cm^2 for one hour while we investigated the (BB) dye photocatalytic breakdown rate at room temperatures.

Fig. 9 displays After 60 minutes of exposure, the highest degradation efficiency of 94.484 percent was attained with 2 milliliters of additional $AgNO_3$, resulting in the best photocatalytic performance. The photolysis efficiency of the remaining nanocatalyst types, on the other hand, declined. Previous research has shown that the amount of Ag loading has a similar effect on photolysis efficiency [40]. Since there is less Ag on the ZnO surface, the Ag/ZnO photolysis efficiency is reduced. Generally, when the load increases, the dispersion of Ag reduces due to the decreased accumulation of certain small particles. Reduced quantity causes weak photoactivity of Ag/ZnO and low efficiency of Ag. The Ag/ZnO photocatalytic degradation efficiency is influenced not only by Ag scattering but also by Schottky barriers that exist between the Ag and ZnO surfaces [41].

CONCLUTION

ZnO (NPs) are effectively produced using a straightforward, efficient, high-yield, and inexpensive mechanochemical combustion process at various calcination temperatures. Since there is less Ag on the ZnO surface, the Ag/ZnO photolysis efficiency is reduced. Generally, when the load increases, the dispersion of Ag reduces due to the decreased accumulation of certain small particles. Reduced quantity causes weak photoactivity of Ag/ZnO and low efficiency of Ag. The Ag/ZnO photocatalytic degradation efficiency is influenced not only by Ag scattering but also by Schottky barriers that exist between the Ag and ZnO surfaces .At 600°C, the photocatalytic activity slightly decreased; the lower photocatalytic activity of Brilliant Blue may be explained by the reduced amount of photo-generated electrons and holes that participated in the reaction .how absorbance efficiency (PDE%) rises to approximately 78% at 500°C after calcination from 55% at 300°C and falls to 75% , impact of adjusting the annealing temperature. It shows that the absorbance efficiency (PDE%) increased from 63% at 300°C to 77% at 400°C, reaching a high of almost 96% at 500°C before declining slightly to roughly 94% at 600°C.

CONFLICT OF INTEREST

The authors declare that there is no conflict of interests regarding the publication of this manuscript.

REFERENCES

1. Alrobayi EM, Algubili AM, Aljeboree AM, Alkaim AF, Hussein FH. Investigation of photocatalytic removal and photonic efficiency of maxilon blue dye GRL in the presence of TiO_2 nanoparticles. Particulate Science and Technology. 2015;35(1):14-20.
2. Maneerung T, Liew J, Dai Y, Kawi S, Chong C, Wang C-H. Activated carbon derived from carbon residue from biomass gasification and its application for dye adsorption: Kinetics, isotherms and thermodynamic studies. Bioresour Technol. 2016;200:350-359.
3. Zhao R, Ma X, Xu J, Zhang Q. Removal of the pesticide imidacloprid from aqueous solution by biochar derived from peanut shell. BioResources. 2018;13(3):5656-5669.
4. Shahul Hameed K, Muthirulan P, Meenakshi Sundaram M. Adsorption of chromotrope dye onto activated carbons obtained from the seeds of various plants: Equilibrium and kinetics studies. Arabian Journal of Chemistry. 2017;10:S2225-S2233.
5. Wang J, Li H, Meng S, Zhang L, Fu X, Chen S. One-pot hydrothermal synthesis of highly efficient SnO_x/Zn_2SnO_4 composite photocatalyst for the degradation of methyl orange and gaseous benzene. Applied Catalysis B: Environmental. 2017;200:19-30.
6. Pascariu P, Airinei A, Olaru N, Olaru L, Nica V. Photocatalytic degradation of Rhodamine B dye using ZnO–SnO_2 electrospun ceramic nanofibers. Ceram Int. 2016;42(6):6775-6781.
7. Kareem NG, Hamid Said M. Syntheses, and Characterization of Complexes Containing Beta-lactam Group with some Transitional Elements and Study their Biological Activity. Neuroquantology. 2021;19(11):72-83.
8. Deng F, Zhao L, Pei X, Luo X, Luo S. Facile in situ hydrothermal synthesis of g-C_3N_4/SnS_2 composites with excellent visible-

light photocatalytic activity. Materials Chemistry and Physics. 2017;189:169-175.
9. Ragi R. Characterization of Synthesis and Biological Studies of Some Transition Metal Complexes of New Schiff Bases of Sulfa Drugs. International Journal of Science and Research (IJSR). 2021;10(12):477-484.
10. Ali I, Said M, AlWazn W. Preparation, Characterization, and Study of Complexes Containing Beta-lactam Group with Some Transitional Elements and their Biological Activity. Egyptian Journal of Chemistry. 2021;0(0):0-0.
11. M. Kamil A, H. Abdalrazak F, F. Halbus A, H. Hussein F. Adsorption of Bismarck Brown R Dye Onto Multiwall Carbon Nanotubes. Journal of Environmental Analytical Chemistry. 2014;01(01).
12. Hameed KAA, Radia ND. Preparation and Characterization of Graphene Oxide (Sodium Alginate-g-polyacrylic Acid) Composite: Adsorption Kinetic of Dye Rose Bengal from Aqueous Solution. Neuroquantology. 2022;20(3):24-31.
13. Şentürk İ, Yıldız MR. Highly efficient removal from aqueous solution by adsorption of Maxilon Red GRL dye using activated pine sawdust. Korean J Chem Eng. 2020;37(6):985-999.
14. Su S, Lu SX, Xu WG. Photocatalytic Degradation of Reactive Brilliant Blue X-BR in Aqueous Solution Using Quantum-sized ZnO. Mater Res Bull. 2008;43(8-9):2172-2178.
15. Karadirek Ş, Okkay H. Ultrasound assisted green synthesis of silver nanoparticle attached activated carbon for levofloxacin adsorption. Journal of the Taiwan Institute of Chemical Engineers. 2019;105:39-49.
16. Agarwal S, Rai P, Gatell EN, Llobet E, Güell F, Kumar M, et al. Gas sensing properties of ZnO nanostructures (flowers/rods) synthesized by hydrothermal method. Sensors Actuators B: Chem. 2019;292:24-31.
17. Rayerfrancis A, Balaji Bhargav P, Ahmed N, Chandra B, Dhara S. Effect of pH on the morphology of ZnO nanostructures and its influence on structural and optical properties. Physica B: Condensed Matter. 2015;457:96-102.
18. Lindsay SM. Statistical mechanics and chemical kinetics. Introduction to Nanoscience: Oxford University PressOxford; 2009. p. 76-132.
19. X. The Bakerian Lecture. —Experimental relations of gold (and other metals) to light. Philos Trans R Soc London. 1857;147:145-181.
20. Removal of Pharmaceutical Amoxicillin drug by using (CNT) decorated Clay/ Fe_2O_3 Micro/Nanocomposite as effective adsorbent: Process optimization for ultrasound-assisted adsorption. International Journal of Pharmaceutical Research. 2019;11(4).
21. Zare M, Namratha K, Alghamdi S, Mohammad YHE, Hezam A, Zare M, et al. Novel Green Biomimetic Approach for Synthesis of ZnO-Ag Nanocomposite; Antimicrobial Activity against Food-borne Pathogen, Biocompatibility and Solar Photocatalysis. Sci Rep. 2019;9(1):8303-8303.
22. Aslan N. Synthesis and Characterization of ZnO@Fe_3O_4 Composite Nanostructures by Using Hydrothermal Synthesis Method. Türk Doğa ve Fen Dergisi. 2022;11(1):95-101.
23. Tan D, Long H, Zhou H, Deng Y, Liu E, Wang S, et al. Effective Photocatalytic Degradation of Methyl Orange Using V2O5@ ZnO Nanocomposite under UV and Visible Irradiations. International Journal of Electrochemical Science. 2020;15(12):12232-12243.
24. Bedano NQ, Alkaim AF. Removal of Pollutants from Aqueous Solutions by using Zinc oxide Nanoparticles. International Journal of Pharmaceutical Quality Assurance. 2022;13(03):108-122.
25. Sharma V, Sharma JK, Kansay V, Sharma VD, Sharma A, Kumar S, et al. The effect of calcination temperatures on the structural and optical properties of zinc oxide nanoparticles and their influence on the photocatalytic degradation of leather dye. Chemical Physics Impact. 2023;6:100196.
26. Nallendran R, Selvan G, Balu AR. CdO-Fe_3O_4 nanocomposite with enhanced magnetic and photocatalytic properties. Materials Science-Poland. 2019;37(1):100-107.
27. Potti PR, Srivastava VC. Comparative Studies on Structural, Optical, and Textural Properties of Combustion Derived ZnO Prepared Using Various Fuels and Their Photocatalytic Activity. Industrial & Engineering Chemistry Research. 2012;51(23):7948-7956.
28. Mhlongo GH, Motaung DE, Nkosi SS, Swart HC, Malgas GF, Hillie KT, et al. Temperature-dependence on the structural, optical, and paramagnetic properties of ZnO nanostructures. Appl Surf Sci. 2014;293:62-70.
29. Omri K, Najeh I, Dhahri R, El Ghoul J, El Mir L. Effects of temperature on the optical and electrical properties of ZnO nanoparticles synthesized by sol–gel method. Microelectron Eng. 2014;128:53-58.
30. Othman AA, Osman MA, Ibrahim EMM, Ali MA. Sonochemically synthesized ZnO nanosheets and nanorods: Annealing temperature effects on the structure, and optical properties. Ceram Int. 2017;43(1):527-533.
31. Yogamalar NR, Srinivasan R, Bose AC. Multi-capping agents in size confinement of ZnO nanostructured particles. Opt Mater. 2009;31(11):1570-1574.
32. Ferdosi E, Bahiraei H, Ghanbari D. Investigation the photocatalytic activity of $CoFe_2O_4$/ZnO and CoFe2O4/ZnO/Ag nanocomposites for purification of dye pollutants. Sep Purif Technol. 2019;211:35-39.
33. Khutso Ntobeng M, Ehi Imoisili P, Jen T-C. Synthesis and photocatalytic performance of Ag-TiVOX nanocomposite. Journal of King Saud University - Science. 2020;32(7):3103-3110.
34. Bau S, Witschger O, Gensdarmes F, Rastoix O, Thomas D. A TEM-based method as an alternative to the BET method for measuring off-line the specific surface area of nanoaerosols. Powder Technol. 2010;200(3):190-201.
35. Kaye BH. Characterization of Powders and Aerosols: Wiley; 1998 1998/12/21.
36. Bourrous S, Ribeyre Q, Lintis L, Yon J, Bau S, Thomas D, et al. A semi-automatic analysis tool for the determination of primary particle size, overlap coefficient and specific surface area of nanoparticles aggregates. J Aerosol Sci. 2018;126:122-132.
37. Wang Z, Cai W, Hong X, Zhao X, Xu F, Cai C. Photocatalytic degradation of phenol in aqueous nitrogen-doped $_{TiO2}$ suspensions with various light sources. Applied Catalysis B: Environmental. 2005;57(3):223-231.
38. Huang Q, Liu S, Wei W, Yan Q, Wu C. Selective synthesis of different ZnO/Ag nanocomposites as surface enhanced Raman scattering substrates and highly efficient photocatalytic catalysts. RSC Advances. 2015;5(34):27075-27081.
39. Sáaedi A, Yousefi R, Jamali-Sheini F, Cheraghizade M, Khorsand Zak A, Huang NM. Optical and electrical properties of p-type Li-doped ZnO nanowires. Superlattices Microstruct. 2013;61:91-96.
40. Ha Pham TT, Vu XH, Dien ND, Trang TT, Kim Chi TT, Phuong PH, et al. Ag nanoparticles on ZnO nanoplates as a hybrid SERS-active substrate for trace detection of methylene blue. RSC advances. 2022;12(13):7850-7863.
41. Liu Y, Zhang Q, Xu M, Yuan H, Chen Y, Zhang J, et al. Novel and efficient synthesis of Ag-ZnO nanoparticles for the sunlight-induced photocatalytic degradation. Appl Surf Sci. 2019;476:632-640.